J Appl Electrochem (2007) 37:583–592
DOI 10.1007/s10800-006-9289-6

ORIGINAL PAPER

Electrochemical oxidation of an acid dye by active chlorine generated using Ti/$Sn_{(1-x)}Ir_xO_2$ electrodes

Flavio H. Oliveira · Marly E. Osugi · Fabiana M. M. Paschoal · Demetrius Profeti · Paulo Olivi · Maria Valnice Boldrin Zanoni

Received: 23 August 2006 / Accepted: 19 December 2006 / Published online: 7 February 2007

Abstract The generation of active chlorine on Ti/$Sn_{(1-x)}Ir_xO_2$ anodes, with different compositions of Ir (x = 0.01, 0.05, 0.10 and 0.30), was investigated by controlled current density electrolysis. Using a low concentration of chloride ions (0.05 mol L^{-1}) and a low current density (5 mA cm^{-2}) it was possible to produce up to 60 mg L^{-1} of active chlorine on a Ti/$Sn_{0.99}Ir_{0.01}O_2$ anode. The feasibility of the discoloration of a textile acid azo dye, acid red 29 dye (C.I. 16570), was also investigated with in situ electrogenerated active chlorine on Ti/$Sn_{(1-x)}Ir_xO_2$ anodes. The best conditions for 100% discoloration and maximum degradation (70% TOC reduction) were found to be: NaCl pH 4, 25 mA cm^{-2} and 6 h of electrolysis. It is suggested that active chlorine generation and/or powerful oxidants such as chlorine radicals and hydroxyl radicals are responsible for promoting faster dye degradation. Rate constants calculated from color decay versus time reveal a zero order reaction at dye concentrations up to 1.0×10^{-4} mol L^{-1}. Effects of other electrolytes, dye concentration and applied density currents also have been investigated and are discussed.

F. H. Oliveira · M. E. Osugi · F. M. M. Paschoal · M. V. B. Zanoni (✉)
Departamento de Química Analítica, Instituto de Química, Universidade Estadual Paulista, Av. Prof. Francisco degni, s/n, C. P. 355, 14801-970 Araraquara, SP, Brazil
e-mail: boldrinv@iq.unesp.br

D. Profeti · P. Olivi
Departamento de Química, Faculdade de Filosofia Ciências e Letras de Ribeirão Preto – USP, 14040-901 Ribeirão Preto, SP, Brazil

Keywords Ti/$Sn_{(1-x)}Ir_xO_2$ anodes · Degradation of azo dye · Dye oxidation · Chlorine generation

1 Introduction

The amount of chorine added to water for disinfection purposes is termed the dose. Some of the added chlorine reacts with organic and inorganic substances in the water. After these reactions occur, the amount of free chlorine that remains in the water is called the residual and is reported in mg L^{-1} or ppm. The final concentration of the residual free chlorine in treated water is around 1.5 mg L^{-1} as required by Brazilian Federal Law [1]. Although the formation of disinfection byproducts in drinking water caused by the reaction between natural organic matter and chlorine or other disinfectants is well known in the literature [2], disinfection processes in water and wastewater treatment systems still rely mainly on chlorine and chlorine-based compounds. Design considerations and operational factors for disinfectant systems that employ chlorine are still being studied in order to optimize these systems. The goal of these studies is to protect public health by inactivating pathogens while still providing an acceptable margin of safety by limiting the generation of disinfection byproducts.

The electrolytic production of chlorine is one of the most important industrial electrochemical reactions [1–3] and is widely used for the disinfection of drinking water [4–9]. In general, the main reaction occurring on a variety of anodic materials [9–21] is the oxidation of chloride ions according to the equation: $2\ Cl^- \rightarrow Cl_2 + 2\ e^-$. Although chlorine gas is the initial product of this reaction, other species can form

depending on the pH of the system. As a result, active chlorine is a term used to refer to the total concentration of all possible chlorine species in water, namely molecular chlorine Cl_2, hypochlorous acid (HOCl) and hypochlorite ions (OCl^-) [6]. All of these strongly oxidizing chlorine species, collectively referred to as active chlorine, are used for electrochemical disinfection. They can be generated electrochemically from natural water that contains ca. 10–250 mg L^{-1} of chloride ions [22–24]. A favorable characteristic of this method is that there is no need to add other chemicals.

In dilute chloride solutions, a parallel reaction occurs on the anode concomitant with the formation of chlorine, i.e., the oxygen evolution reaction (OER) [20–22]. As solution to improve the method the selection of dimensionally stable anodes (DSA®) has become very popular. These electrodes are thermally prepared oxide electrodes for which a titanium substrate is covered by metallic oxides such as TiO_2, IrO_2, SnO_2, RuO_2 and Ta_2O_3 [7, 8, 16–21, 25–27]. These DSA® electrodes provide good catalytic activity, mechanical and chemical stability under high positive potential, good resistance to corrosion, and high current efficiency for the oxidation of chloride ions.

The use of DSA® for the indirect degradation of organic pollutants is an active area of research [28, 29]. In general, the electrochemical degradation of organic compounds (R) on metal oxide electrodes M_{ox} appears to involve the generation of $OH^{\cdot}$ radicals on the surface of the electrodes (M_{ox} ($\cdot$OH)), as shown by the following equations:

$$M_{ox} + H_2O \rightarrow M_{ox}\,(\cdot OH) + H^+ + e^- \quad (1)$$

$$R + M_{ox}\,(\cdot OH) \rightarrow CO_2 + z\,H^+ + M_{ox} + z\,e^- \quad (2)$$

Among the several DSAs that are available for degrading organics, tin dioxide anodes are often used to oxidize organic pollutants [28–33]. This material can be employed because it is characterized by high oxygen overpotential and, more significantly, a large accumulation of $OH^{\cdot}$ radicals on its surface. Studies with SnO_2 electrodes supported on titanium indicate that such electrodes are useful for the electrochemical decomposition of stable species [30–32]. It has also been shown that addition of RuO_2 increases the electrode service life and decreases the water discharge potential [31].

In recent years [25, 26] some authors have pointed out that several other radicals ($Cl^{\cdot}$, $ClO^{\cdot}$ and $Cl_2^{\cdot}$) can be formed during chlorine generation, which have higher oxidation potentials (E^0 $Cl^{\cdot}/Cl^-$ = 2.410 V vs. NHE and E^0 $Cl_2^{\cdot}/2Cl^-$ = 2.090 V vs. NHE) than active chlorine (E^0 $Cl_2/2Cl^-$ = 1.395V vs. NHE) [33]. Therefore, the possible occurrence of these other chlorine radicals on DSA, generated analogously to hydroxyl radicals during the electrocatalytic oxidation of chloride ions, might increase the oxidation strength of active chlorine for the indirect degradation of organic pollutants.

The present work evaluates the ability of $Ti/Sn_{(1-x)}Ir_xO_2$ DSAs with different compositions of Ir (x = 0.01, 0.05, 0.10 and 0.30) to generate active chlorine by the electrocatalytic oxidation of chloride solution. In addition, the feasibility of using this approach to bleach an acid dye [34] by indirect generation of chlorine was studied to determine if this method was suitable for treating such dyes. Acid red 29 (chromotrope 2R) (Fig. 1) was chosen as a model acid dye because of its wide use in the leather industry. The effect of using anodes with different compositions on the degradation rate of the dye was determined. Then this electrocatalytic method was optimized for effluents similar to those that occur in the leather industry that contain chloride as a residue.

2 Experimental section

The content of free chlorine dissolved in solution was determined by the DPD (*N*,*N*,-diethyl-*p*-phenylenediamine) colorimetric method [24] calibrated previously to a minimum detectable concentration of chlorine of 10 μg L^{-1}. Aliquots of 150 μL of the photo-electrolyzed solution were collected in a tube containing

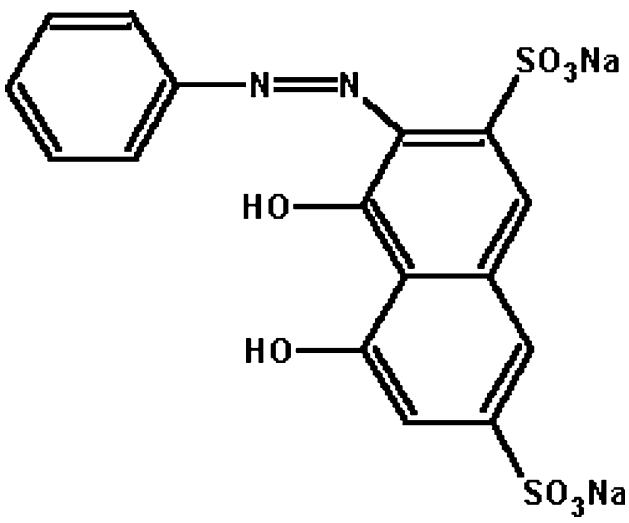

Fig. 1 Chemical structure of acid red 29 dye

phosphate buffer and DPD solution. The product of the instantaneous reaction between free chlorine and DPD indicator produced a red color which was analyzed immediately by measuring the absorption spectra in the visible range of 400–800 nm with a Hewlett Packard spectrophotometer, model HP 8452A, in a 10-mm quartz cell. The concentration of chlorine (mg L^{-1}) in solution was determined by measuring the absorbance at 512 nm using a calibration curve prepared previously with potassium permanganate solution as recommended [24]. Samples of dye solution were also analyzed using spectrophotometric analysis and recording the respective spectra from 190 nm to 800 nm for aliquots removed each 5 min.

Total organic carbon (TOC) and color removal were monitored using a Total Organic Carbon Analyzer (Shimadzu 500A) and a diode array UV–Vis spectrophotometer (HP 8453). Spectra were recorded over a wavelength range from 190 nm to 800 nm in a quartz cell.

Electrochemical measurements were performed using a Potentiostat/ Galvanostat (EG&G PARC model 283) controlled by Electrochemical 270 software operating in galvanostatic mode at low current densities of 5, 10 and 25 mA cm^{-2}. A two-electrode cell with one compartment was used for cyclic voltammetry experiments. The working electrodes were $Ti/Sn_{(1-x)}Ir_xO_2$ anodes (geometric surface area of 1.28 cm^2) with different compositions of Ir (x = 0.01, 0.05, 0.10 and 0.30) and a platinum gauze cathode. The $Ti/Sn_{(1-x)}Ir_xO_2$ electrodes were prepared using a mixture of precursor solutions [35]. The tin precursor solution was prepared by dissolution of tin citrate in citric acid/ethylene glycol solution maintaining the molar ratio metal:citric acid:ethylene glycol 1:3:10. The iridium chloride (1 g/10 mL) was prepared by dissolution in either 50% HCl (v/v) and subsequent addition of ten drops of 30% H_2O_2 (m/v). The final solution was obtained by mixing the appropriate mass of both precursor solutions to obtain the desired composition. The thin films were prepared on previously sandblasted Ti plates (1.0 × 1.0 cm), pre-treated for 10 min in heated 10% oxalic acid solution. The precursor solutions were applied onto the substrate by brushing and heated at 100 °C for 5 min, and at 550 °C for 5 min. This procedure was repeated until a mass corresponding to a nominal thickness of 2 μm (nonporous) was obtained. When this condition was achieved, the electrodes were calcinated at 550 °C for 1 h, in air atmosphere. A detailed description of the preparation method can be found elsewhere [36].

3 Results and discussion

3.1 Chloride oxidation on $Ti/Sn_{(1-x)}Ir_xO_2$ anodes

Initially, the influence of the composition of the anode on the generation of chlorine was investigated by monitoring the electrochemical oxidation of 20 mL of 0.05 mol L^{-1} of chloride ions on $Ti/Sn_{0.99}Ir_{0.01}O_2$ (Curve A); $Ti/Sn_{0.95}Ir_{0.05}O_2$ (Curve B); $Ti/Sn_{0.90}Ir_{0.1}O_2$ (Curve C); $Ti/Sn_{0.70}Ir_{0.30}O_2$ (Curve D) anodes at current density of 25 mA cm^{-2} over a period of 40 min. Results are shown in Fig. 2. To obtain these data, aliquots of the electrolyzed sample were removed each 5 min during the electrolysis and analyzed immediately by the DPD colorimetric method to determine the

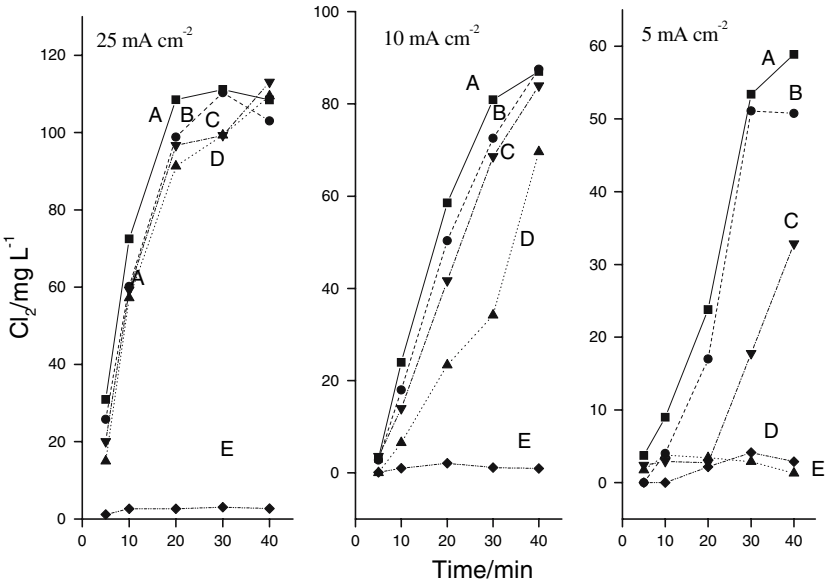

Fig. 2 Influence of the anode material on the generation of chlorine by the electrochemical oxidation of 0.05 mol L^{-1} NaCl on $Ti/Sn_{0.99}Ir_{0.01}O_2$ (Curve A); $Ti/Sn_{0.95}Ir_{0.05}O_2$ (Curve B); $Ti/Sn_{0.90}Ir_{0.1}O_2$ (Curve C); $Ti/Sn_{0.70}Ir_{0.30}O_2$ (Curve D) and graphite electrode (E). Tests were performed for 40 min of electrolysis at current densities of 25, 10 and 5 mA cm^{-2}

amount of active chlorine generated as a function of time. The results show that active chlorine production is faster during the initial stage of the process and then reaches a maximum value after a longer period of time, suggesting that maximum saturation has been attained in addition to the expected limitations imposed by the geometric area of the electrode or the solubility of chlorine gas in the solution. Because chlorate may be generated by parasitic reactions of hypochlorite in solution [2, 25] and on the anode: [$6\ OCl^- + 3\ H_2O \rightarrow 2\ CLO_3^- + 6\ H^+ + 4\ Cl^- + 1.5\ O_2 + 6\ e^-$] and [$2\ HOCl + OCl^- \rightarrow ClO_3 + 2\ H^+ + 2\ Cl^-$], the sample was analyzed by reaction with phosphoric acid and Mn (II) to identify possible chlorate formation [37]. Under the optimized conditions of these experiments, chlorate was not detected, suggesting that parasitic reactions of hypochlorite are minimized in this process.

For comparison the performance obtained on graphite electrode is shown in Fig. 2, Curve E. As expected, the production of active chlorine is much higher for DSA electrodes under all conditions. Oxide electrodes containing any amount of Ir displayed enhanced electrocatalytic activity in comparison with graphite, and all oxide electrodes produced similar amounts of active chlorine at a current density of 25 mA cm^{-2}. Amounts of around 100 mg L^{-1} of active chlorine can be generated after 20 min of electrolysis on a $Ti/Sn_{0.90}Ir_{0.1}O_2$ electrode, suggesting that the method could be used for water disinfection, since the permanent level of chlorine in solution has to be maintained at 1.5 mg L^{-1}.

Nevertheless, the set of curves obtained for the same electrodes at low current densities of 10 and 5 mA cm^{-2} (Fig. 2) indicates that the performance of $Ti/Sn_{(1-x)}Ir_xO_2$ electrodes changes dramatically as the iridium composition changes from $x = 0.01$ to 0.3. Both graphs indicate that maximum chlorine production is obtained by incorporating a small quantity of iridium in its composition (Curve A, Fig. 2). This values decreases proportionally with iridium composition, and the electrode containing 30% iridium provides the lowest rate of chloride ion oxidation.

In order to evaluate the effect of electrode composition on the rate of chlorine generation, the initial rate of electrocatalytic oxidation of chloride ions for each current density was calculated assuming zero-order kinetics (i.e., a linear relationship of C vs. t). Values of these rate constants and associated anodic current efficiencies are shown in Table 1. At a low current density of 5 mA cm^{-2}, the rate of active chlorine production increases at least 10 times when the composition of iridium is increased from 1% to 30% and at least 100 times in relation to the graphite electrode. These results indicate that it is possible to promote oxidation of small amounts of chloride ions even at current densities as low as 5 mA cm^{-2}. As expected, at a higher current density of 25 mA cm^{-2}, the rate of conversion of chloride ions is almost constant, and the influence of iridium is not so pronounced.

The importance of iridium composition is better evaluated by calculating the faradaic efficiency for each electrode (also shown in Table 1). The values of faradaic efficiency for the chlorine evolution reaction were calculated using the equation:

$$\eta = (2\ F\ [Cl_2]\ V)/(I\ t)\ \times\ 100\%,$$

where V is the volume of solution (mL), F is Faraday's constant, $[Cl_2]$ is the concentration of active chlorine (mg L^{-1}), I is the applied current (A), and t is the electrolysis time (s) for each tested anode. These values are expressed as percentages in Table 1.

As expected at 25 mA cm^{-2} current density, the faradaic efficiencies for chlorine evolution on the DSAs were around 25% but this value was much lower for the graphite electrode. On the other hand, at 5 mA cm^{-2} current density, the highest faradaic

Table 1 Effect of electrode composition on the generation of active chlorine rate (k) and anodic current efficiency (η) for oxidation of 0.05 mol L^{-1} sodium chloride under current density of 5, 10 and 25 mA cm^{-2}

Current density	5 mA cm^{-2}			10 mA cm^{-2}			25 mA cm^{-2}		
Eletrode type	K/mg L^{-1} min^{-1}	η/%	E/V	K/mg L^{-1} min^{-1}	η/%	E/V	K/mg L^{-1} min^{-1}	η/%	E/V
Graphite	6.5×10^{-3}	4.7	–	1.7×10^{-2}	1.2	–	1.6×10^{-2}	7.0	–
$Ir_{1\%}$	1.1×10^{-1}	67	0.33	1.3×10^{-1}	56	0.32	8.3×10^{-2}	25	0.32
$Ir_{5\%}$	6.7×10^{-2}	58	0.29	4.7×10^{-2}	50	0.20	8.4×10^{-2}	25	0.04
$Ir_{10\%}$	4.5×10^{-2}	38	0.26	7.4×10^{-2}	39	0.19	1.2×10^{-1}	25	0.04
$Ir_{30\%}$	1.2×10^{-2}	37	0.27	5.8×10^{-2}	47	0.20	1.0×10^{-1}	26	0.04

K = active chlorine production rate

E = cell potential measured during 10 min of electrolysis

*Anode = $Ti/Sn_{(1-x)}Ir_{x\%}O_2$

efficiency was obtained with the $Ti/Sn_{0.99}Ir_{0.01}O_2$ anode and the faradaic efficiency decreased as the iridium content increased. This trend was also observed for the electrolysis carried out at 10 mA cm^{-2}, with the exception for $Ti/Sn_{0.70}Ir_{0.30}O_2$ anode.

These results suggest that tin oxide exhibits a high overpotential for the oxygen evolution reaction (OER). For this reason, generation of chlorine at lower potentials should be preferred on these DSAs. However, the addition of iridium to these electrodes increases their durability and so can also influence the chlorine generation. The good performance of SnO_2 electrodes containing small quantities of iridium at low current densities of 5 and 10 mA cm^{-2} indicates that chlorine generation is preferential on these electrodes, most likely due to minimization of the competitive OER. On the other hand, at a high current density of 25 mA cm^{-2}, the Ir content does not affect markedly the generation of chlorine. In this case, the high overpotential for chlorine generation under this operating condition favors the OER even with electrodes that contain smaller amounts of iridium. Therefore, the faradaic efficiencies and initial rates of chlorine generation are similar for all anodes at this current density.

In order to determine if the electrode materials interfere with the oxidation of chloride ions, a series of voltammograms were recorded for $Ti/Sn_{(1-x)}Ir_xO_2$ electrodes in 0.05 mol L^{-1} of Na_2SO_4 and 0.05 mol L^{-1} of NaCl. Figure 3 exhibits the representative behavior observed for $Ti/Sn_{0.7}Ir_{0.3}O_2$ (Curve I) and $Ti/Sn_{0.99}Ir_{0.01}O_2$ (Curve II). Figure 3 (Curve I) indicates that the oxygen evolution reaction (25) is retarded on $Ti/Sn_{0.99}Ir_{0.01}O_2$, while the formation of NaCl is preferential. In addition, the currents observed for chlorine generation is higher on the $Ti/Sn_{0.99}Ir_{0.01}O_2$ than the currents obtained for the other compositions (Fig. 3 (Curve II). It is well known from the literature [36, 38] that electrodes based on SnO_2 present higher overpotential for OER. Therefore, $Ti/Sn_{0.7}Ir_{0.3}O_2$ electrodes have shown a shifting of the OER curve to less positive potentials. The chlorine evolution reaction may occur concomitantly with the OER on these electrodes with high amount of Ir higher than 0.5%. This hypothesis is confirmed by the anodic faradaic efficiency presented in Table 1, which low values are obtained for electrodes containing higher than 5% of Ir and the respective anode potential measured during 10 min of electrolysis. The cell potential generated during electrolysis of chloride on anodes (1% Ir) is always higher than the other anodes, but the effect is minimized at high current density when the overpotential is reached for both OER and chlorine evolution.

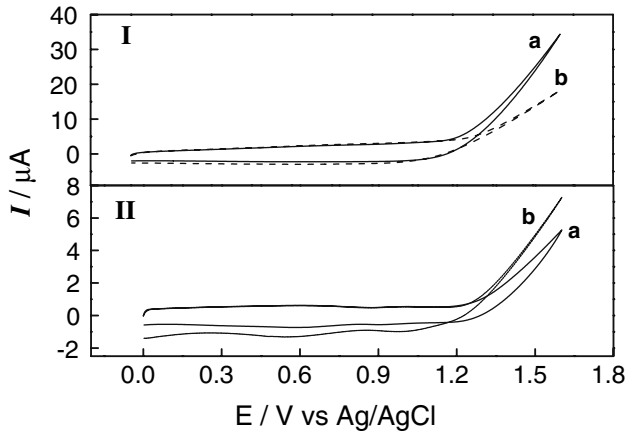

Fig. 3 Cyclic voltammograms on $Ti/Sn_{0.99}Ir_{0.01}O_2$ (I) and $Ti/Sn_{0.7}Ir_{0.3}O_2$ (II) anodes in 0.05 mol L^{-1} NaCl (a) and 0.05 mol L^{-1} Na_2SO_4 (b). Scan rate = 50 mV s^{-1}

It was observed by Ortiz et al. [36] that the mechanism of chlorine evolution may change on $Ti/(SnO_2 + IrO_2)$ electrodes containing less than 10% Ir due to the semiconducting nature of the oxide layer which increases the layer resistance. The activation of SnO_2 electrodes at voltages between 0.9 V and 1.3 V vs. SCE in the presence of chloride ions was explained by Cachet et al. [38] as caused by a corrosion mechanism involving the breaking of Sn–O surface bonds that increases the activity of SnO_2 electrodes. The mechanisms proposed by Ortiz et al. [36] and by Cachet et al. [38] suggest the formation of a $Cl^{\cdot}$ radical as an initial step in chlorine evolution.

The $Sn_{(1-x)}Ir_xO_2$ coating containing a small amount of iridium displays better electrode durability when compared with a pure SnO_2 electrode as well as a reasonable rate of chlorine evolution. Therefore, this electrode could potentially be suitable for different applications of chlorine-mediated electro-oxidation. Since chlorine evolution was clearly electrocatalyzed by all of the $Ti/Sn_{(1-x)}Ir_xO_2$ tested electrodes and it is known [25] that several other radicals can also be formed in solutions containing active chlorine compounds in the presence of a catalyst, the present system was tested as a possible electrochemical method for the degradation of an acid dye. This dye was chosen to serve as a model of an organic pollutant.

3.2 Indirect oxidation of acid red 29 dye on $Ti/Sn_{(1-x)}Ir_xO_2$ anodes

UV–Vis spectra obtained before and after the electrolysis of 4.0×10^{-5} mol L^{-1} acid red 29 dye (AR29) in 0.05 mol L^{-1} solutions of NaCl on $Ti/Sn_{0.99}Ir_{0.01}O_2$ anodes are exhibited in Fig. 4. The current density was 25 mA cm^{-2}. This degradation process significantly

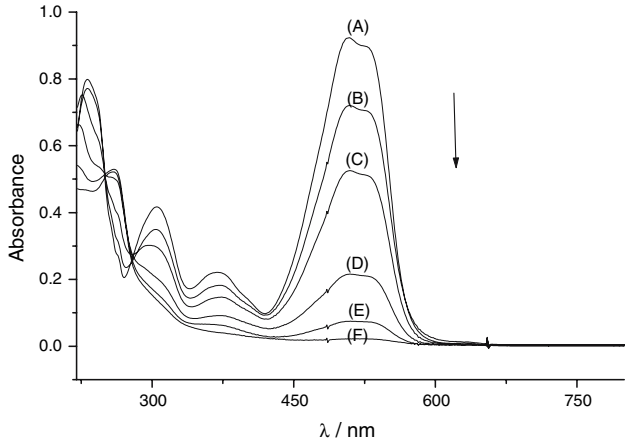

Fig. 4 UV–Vis spectra representing the degradation of 4.0×10^{-5} mol L^{-1} acid red 29 R in 5.0×10^{-2} mol L^{-1} NaCl during electrolysis on a $Ti/Sn_{0.99}Ir_{0.1}O_2$ anode at a current density of 25 mA cm^{-2}. (A) 0 min (B) 1 min (C) 2 min (D) 3 min (E) 4 min (F) 5 min

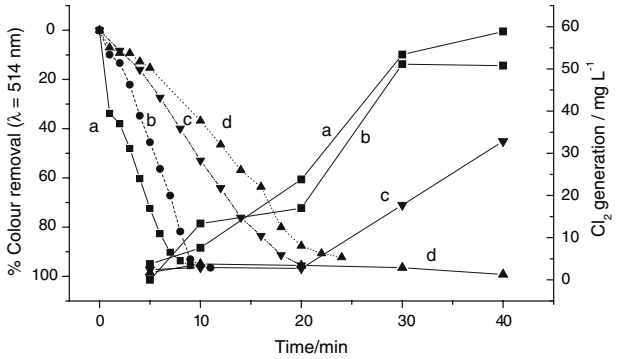

Fig. 5 Effect of the electrocatalytic materials on the color removal of a 4.0×10^{-5} mol L^{-1} AR29 dye solution in 0.05 mol L^{-1} NaCl electrolyzed at 5 mA cm^{-2} (left). The generation of active chlorine under the same experimental conditions but without the dye is also shown (right). Both sets of experiments with all $Sn_{(1-x)}Ir_xO_2$ anodes with Ir = 1% (a); 5% (b); 10% (c) and 30% (d)

modifies the chemical structure of AR29 dye, as shown by the total suppression after 5 min of electrolysis of the absorbance peaks at 530, 514 and 371 nm. These changes were attributed to changes in the chromophore group in the dye (azo group). In addition, the intensities of the bands at 307 and 229 nm decrease greatly, mainly attributed to changes in centers with aromatic character in the dye molecule [34]. On the other hand, the spectrum obtained after 4 min of electrolysis displayed a small absorbance peak at 264 nm. This absorbance peak remained at this wavelength but slowly lost intensity, necessarily implying that a transient species formed during the fragmentation of the dye molecule and that this species required a longer time to react. In practice, this species completely disappeared after 120 min of electrolysis. The residual peak at 300 nm is associated with an excess of chlorine generated during the process. When this experiment was repeated using sodium sulfate as the supporting electrolyte, there was no color removal. Therefore, the de-colorization process is probably occurring in the bulk solution via generated chlorine reacting with the dye molecule.

The effect of current density on the electrocatalytic bleaching of AR29 dye solution was evaluated by comparing the rates of color removal at current densities of 5, 10 and 25 mA cm^{-2} in 0.05 mol L^{-1} NaCl solution for all four anodes. Figure 5 presents the color removal of a 4.0×10^{-5} mol L^{-1} AR29 dye solution during electrolysis at 5 mA cm^{-2} as well as the respective chlorine generation under the same experimental conditions but without the dye. At this dye concentration, the time required to reach 100% bleaching increases from 10 min to 25 min when the Ir composition increases from 1% to 30%. This behavior may be related to chlorine generation, since the electrodes containing more Ir produce less chlorine than electrodes richer in Sn. The time required for complete electrolytic removal of the dye coincides with the time required to form at least 4 mg L^{-1} of active chlorine in the bulk solution.

Electrolysis carried out at current densities of 10 mA cm^{-2} (Fig. 6, curves a–d) yielded complete color removal in 12 min only for the electrode containing 1% Ir. At the higher current density of 25 mA cm^{-2}, faster bleaching was obtained as shown in Fig. 6, curves (e–I). After 12 min of electrolysis at the higher current density, there was complete color

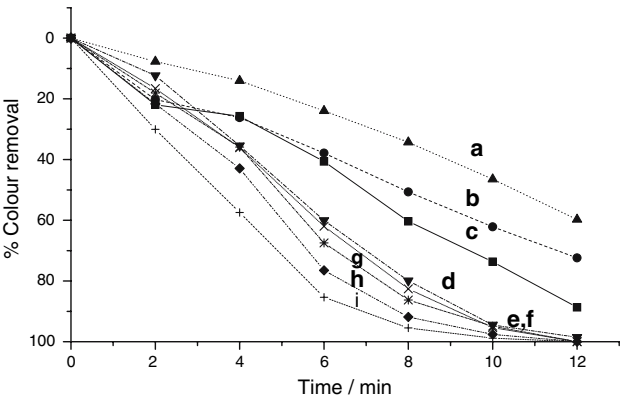

Fig. 6 Effect of electrolysis time on the removal of colour obtained for 4.0×10^{-5} mol L^{-1} AR29 dye in 5.0×10^{-2} mol L^{-1} NaCl electrolyzed on $Sn_{(1-x)}Ir_xO_2$ anodes under two current densities. At 10 mA cm^{-2}: -■- 1% (d), -●- 5% (c), -▲- 10% (b), -▼- 30% (a). At 25 mA cm^{-2}: -■- 1% (i), -●- 5% (h), -▲- 10% (f), -▼- 30% (e)

removal from the solution. As demonstrated previously, these results reflect the time required for generation of chlorine, since the bleaching of the dye solution is occurring indirectly by reaction with active chlorine generated on the electrode surface. The increase in current density did not significantly affect the time required for color removal when the electrodes contained a small amount of Ir. However, this time is drastically reduced when electrodes richer in Ir are employed. In the case of $Ti/Sn_{0.7}Ir_{0.3}O_2$ electrodes, the time required for complete color removal decreased from 25 min, when a 5 mA cm^{-2} current density was applied, to 12 min for 25 mA cm^{-2}.

In order to determine the effect of pH on the rate of bleaching of AR29 dye, electrolysis experiments were performed using the $Ti/Sn_{0.99}Ir_{0.01}O_2$ electrode operating at a current density of 25 mA cm^{-2} in a solution containing 1×10^{-4} mol L^{-1} of dye and 0.15 mol L^{-1} of NaCl at pH 2–12. The results are presented in Fig. 7. Complete discoloration of the dye solution was obtained at pH values lower than 8 but the rate of degradation was higher at pH values less than 4, where 100% removal of color was observed after only 3 min of electrolysis. On the other hand, at pH 12 only 50% of color was removed after 7 min of electrolysis.

In agreement with the literature [22–24], the overall concentration of dissolved chlorine available after the chlorination process is called active chlorine and is given by the summation of three possible species: chlorine (Cl_2), hypochlorous acid (HOCl) and hypochlorite ion (OCl^-). The relative amount of each of these free chlorine forms is pH and temperature dependent. At room temperature and 1.0 mmol L^{-1} of chloride, $Cl_2(aq)$ is the dominant species under very acidic conditions, HOCl predominates due to hydrolytic disproportionation at 3.3 < pH < 7.5, while OCl^- is the main species at pH > 7.5. Control over pH can be a critical factor in determining the degree of disinfection achieved by a certain level of free chlorine because the disinfecting ability of hypochlorous acid is generally regarded to be larger (80 to 100 times) than that of hypochlorite ion. Thus, this behavior clearly indicates that in acidic media, where either chlorine gas or hypochlorous acid predominate, faster degradation of the dye solution is obtained. Although these species have higher oxidation potentials than hypochlorite ions, under acidic conditions competing reactions such as chlorate and perchlorate generation [6] can occur and are disadvantageous. On the other hand, the dramatic decrease in the rate of discoloration of the dye solution at pH 12 is probably due to the increased generation of oxygen associated with the OER, which renders chlorine formation more difficult. Further studies of the indirect oxidation of acid red 29 dye were performed at an initial pH of 4 in order to obtain fast conversion of chloride into active chlorine without the need to further adjust the pH. This condition assures that the rate of degradation of the dye will be quite rapid.

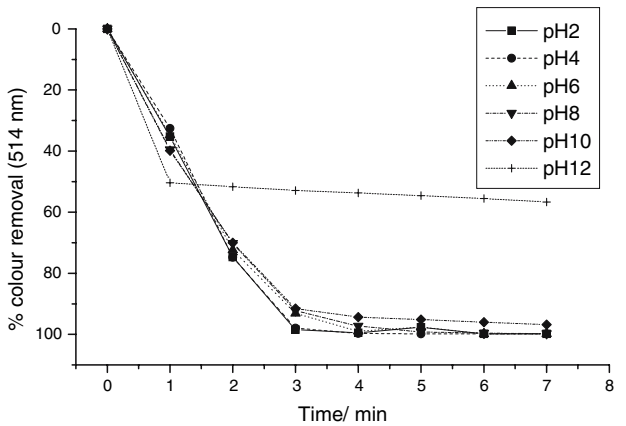

Fig. 7 Effect of pH variation on the discolouration of 1.0×10^{-4} mol L^{-1}AR29 dye in 0.15 mol L^{-1} of NaCl electrolyzed at current density of 25 mA cm^{-2} using $Ti/Sn_{0.9}Ir_{0.1}O_2$ anode

In order to investigate the influence of the initial concentration of chloride ion on the indirect oxidation of AR29 dye via chlorine generation, the $Ti/Sn_{0.99}Ir_{0.01}O_2$ anode was used to electrolyze 7.5×10^{-5} mol L^{-1} of AR29 dye in either 0.05 mol L^{-1} of NaCl or 0.15 mol L^{-1} of NaCl. These experiments were performed at an initial pH of 4.0 and a current density of 25 mA cm^{-2}. The electrocatalytic decomposition of the AR29 was followed by measuring the absorbance decay at a wavelength of 514 nm over 30 min. Increasing the initial concentration of chloride ion was observed to increase the rate of oxidation of the dye. The rate of oxidation appeared to follow zero order kinetics, as shown in Fig. 8. Rate constants calculated from the resulting linear relationships were 2.35×10^{-2} mg L^{-1} min^{-1} for 0.05 mol L^{-1} of chloride ions and 9.24×10^{-2} mg L^{-1} min^{-1} for 0.15 mol L^{-1} of chloride ions. This behavior is typical for a zer-order reaction in dye consumption.

The effect of the initial concentration of the dye on its rate of discoloration was investigated over the range of 4.0×10^{-5} mol L^{-1} to 7.5×10^{-4} mol L^{-1} of AR19, while fixing the initial concentration of chloride ion at 0.15 mol L^{-1} and maintaining a current density of 25 mA cm^{-2}. The results are shown in Fig. 9. At concentrations less than 1×10^{-4} mol L^{-1} of AR29 dye, complete discoloration was achieved after 3 min of electrolysis, with the reaction appearing to be zero order. Although the amount of active chlorine generation should have been constant in all the experiments,

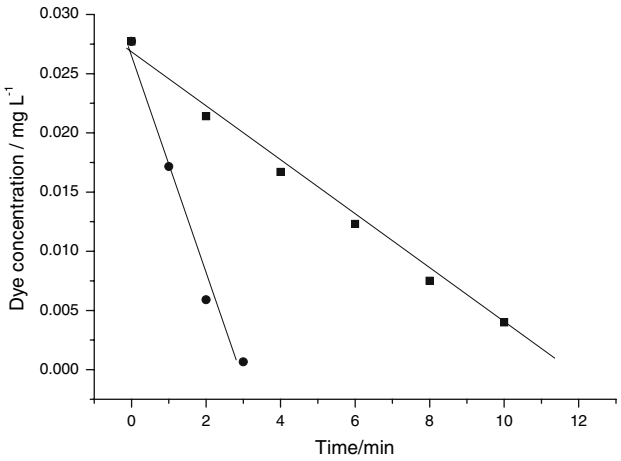

Fig. 8 Effect of the initial concentration of chloride ion on the degradation of 7.5×10^{-5} mol L^{-1} AR29 dye in either 0.05 mol L^{-1} NaCl (A) or 0.15 mol L^{-1} NaCl (B). The initial pH was 4.0 and I = 25 mA cm^{-2}

it took longer to achieve discoloration when the AR29 dye concentration exceeded 1×10^{-4} mol L^{-1}, as shown in curves d and e. These results suggest that the dye degradation rate depends on the [NaCl]/[dye] ratio, with low dye concentrations requiring low NaCl concentrations.

Using the best conditions for electrocatalytic oxidation, an experiment was conducted to measure the change in the concentration of total organic carbon in the dye solution during electrocatalytic oxidation. This test was performed over a 4-h period using 7.5×10^{-5} mol L^{-1} of AR29 in 0.15 mol L^{-1} of NaCl and a $Ti/Sn_{0.99}Ir_{0.01}O_2$ anode at a current density of 25 mA cm^{-2}. Results from the TOC measurements are given in Fig. 10A. Several replicate experiments demonstrated that complete discoloration occurred after a few minutes of treatment but that longer times were needed to promote mineralization of the dye. Although 64% of the TOC was mineralized relatively rapidly during the first 2 h of electrolysis, the rate of mineralization decreased significantly after that, reaching a maximum of 70% removal of TOC after 4 h.

The results indicate that the degradation of AR29 dye could be occurring due to the generation of active chlorine (Cl_2, HClO, ClO^-) and chorine radicals ($Cl^{\cdot}$, $Cl_2^{\cdot}$) that are powerful oxidizing species. On the other hand, $OH^{\cdot}$ radicals should also be generated on the DSA. Both situations would lead to the formation of powerful oxidizing agents capable of degrading the acid dye.

In order to confirm this hypothesis, the previous experiment was repeated using 0.15 mol L^{-1} of Na_2SO_4 instead of NaCl. UV–Vis absorbance spectra obtained at different times during 4 h of electrolysis in the sulfate medium are shown in Fig. 11. Total organic carbon removal of the electrolyzed solution was also monitored and is shown in Fig. 10B. The results indicate that color removal occurred slowly in the sulfate medium, reaching a maximum discoloration of 67% after 6 h of electrolysis. In addition, only 20% mineralization was observed when the electrolysis was performed in the sulfate medium. These results suggest that the electrolytic process involves only partial cleavage of the dye molecule when active chlorine species are not generated.

A remarkable difference in the UV–Vis spectra was observed when the dye solution was bleached by

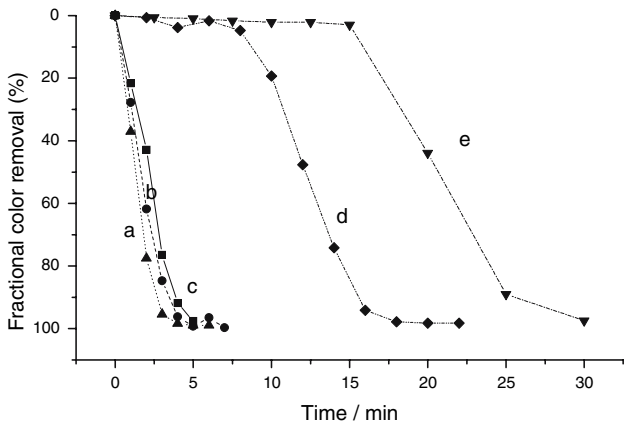

Fig. 9 Effect of the initial concentration of the dye on its degradation at I = 25 mA cm^{-2} on a $Ti/Sn_{0.99}Ir_{0.01}O_2$ anode in 1.5×10^{-1} mol L^{-1} NaCl. Dye concentration: (■, a) 4.0×10^{-5} mol L^{-1}; (▲, b) 7.5×10^{-5} mol L^{-1}; (●, c) 1.0×10^{-4} mol L^{-1}; (◆, d) 5.0×10^{-4} mol L^{-1}; and (▼, e) 7.5×10^{-4} mol L^{-1}

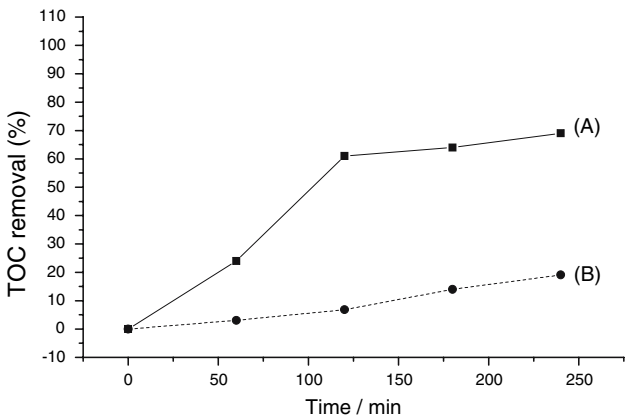

Fig. 10 Total organic carbon removal during the electrocatalytic treatment of 1×10^{-4} mol L^{-1} AR29 dye in 1.5×10^{-1} mol L^{-1} NaCl (A) over a $Ti/Sn_{0.99}Ir_{0.1}O_2$ anode at I = 25 mA cm^{-2}. This experiment was repeated in 1.5×10^{-1} mol L^{-1} Na_2SO_4 (B)

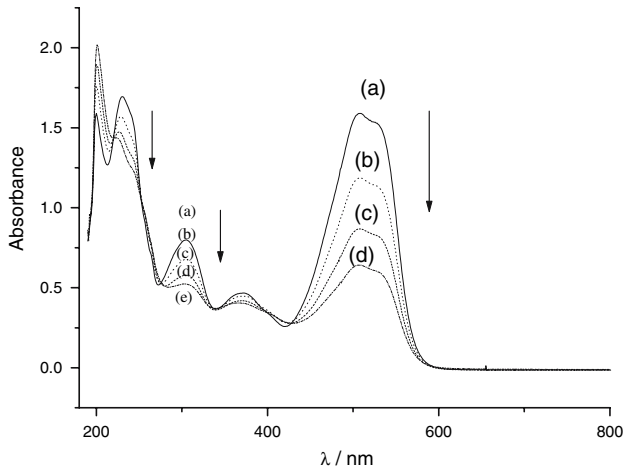

Fig. 11 UV–Vis absorbance spectra for the system shown in Fig. 10B. Electrolysis time: (a) 60 min (b) 120 min (c) 240 min (d) 300 min (e) 360 min

bubbling free chlorine generated by a chemical method into the test solution employed above. Absorbance bands in the visible region of the spectrum rapidly disappeared, although there was a negligible difference in the removal of total organic carbon, indicating that there was only limited mineralization of the dye molecule.

Therefore, it appears that, as chlorine radicals are better oxidants than only active chlorine species, mineralization of the original dye is more efficient when an electrocatalytic oxidation process is used under conditions that can generate chlorine radicals. Although hydroxyl radicals could also participate in the process, their effect is less important under optimized experimental conditions. The rapid discoloration and mineralization observed in the chloride medium probably occur due to the formation of chlorine radicals.

Although the reaction mechanism for the electrochemical oxidation of this model organic compound is complex, these results are in agreement with the literature in that the oxidation reaction of AR29 dye on a SnO_2 anode initially involves chlorine radicals produced by the electrochemical oxidation of chloride ions on the electrode surface. The formation of $Cl^{\cdot}$ radicals in the system leads subsequently to more complete mineralization of the organic species than would be expected in conventional chlorination. However, the possible formation and adsorption of $OH^{\cdot}$ radicals on the electrode surface can also lead to oxygen formation and a subsequent decrease in the efficiency of electrolysis.

Although this electrocatalytic process seems to be suitable for the discoloration of acid dyes, the possibility of forming disinfection byproducts during this process needs to be considered. Initial qualitative tests for the formation of chloramine compounds were negative but further studies are in progress.

4 Conclusion

This study demonstrates that $Ti/Sn_{(1-x)}Ir_xO_2$ electrodes may have practical applications for chlorine production. The use of $Ti/Sn_{0.99}Ir_{0.01}O_2$ anodes offered a simple and precise methodology to convert chloride ions into chlorine. This approach has economic potential since these systems operate at low current densities but provide high faradaic efficiencies. The electrocatalytic oxidation of chloride ions appears to involve the formation of chlorine radicals, which then leads to rapid and complete discoloration of Acid red 29 dye with significant mineralization of the dye (70%) after 4 h of treatment.

Acknowledgements The authors thank Dr. Walt Zeltner of the University of Wisconsin for English language revision of this paper and acknoledge financial support from Brazilian funding agencies CAPES, CNPq and FAPESP.

References

1. Brasil (2004) Portaria 518, Ministério da Saúde, issued in 03/25/2004 and published in DOU Executivo in 03/26/2004
2. Xie YF (2004) Disinfection byproducts in drinking water, formation, analysis and control. CRC Press LLC
3. Burney HS (1993) In: White RE, Conway BE, Bockris JOM (eds) Modern aspects in electrochemistry. Plenum Press, New York, p 393
4. Rudolf M, Rousar I, Krysa J (1995) J Appl Electrochem 25:155
5. Rengarajan V, Sozhan G, Narasimham KC (1996) Bull Electrochem 12:327
6. Casson LW, Bess JW Jr (2003) Conversion to on-site sodium hypochlorite generation, water and wastewater application. CRC Press LLC
7. Kraft A, Stadelmann M, Blaschke M, Kreysig D, Sandt B, Schroder F, Rennan J (1999) J Appl Electrochem 29:861
8. Kraft A, Blaschke M, Kreysig D, Sandt B, Schroder F, Rennan J (1990) J Appl Electrochem 29:895
9. Patermarakis G, Fountoukidis E (1990) Water Res 24:1491
10. Schoberl M (1991) Eur Pat EP 0 515 628 B1
11. Kanekuni N, Shono N, Kyohara M, Tabata K, Kono S, Hayakawa M (1995) Eur Pat Appl EP 0 711 730 AL
12. Ibl N, Vogt H (1981) In: Bockris JOM, Conway BE, Yeager E, White RE (eds) Comprehensive treatise of electrochemistry, vol 2. Plenum Press, New York, p 167
13. Bennett JE (1974) Chem Eng Prog 70:60
14. Arikado T, Iwakura C, Tamura H (1978) Electrochim Acta 23:9
15. Harrison JA, Hermijanto AD (1987) J Electroanal Chem 225:159
16. Do JS, Yeah WC (1995) J Appl Electrochem 251:483

17. Czarnetzki LR, Janssen LJJ (1992) J Appl Electrochem 22:315
18. Do JS, Yeah WC, Chao IYa (1997) Ind Eng Chem Res 36:349
19. Rudolf M, Rousar I, Krysa J (1995) J Appl Electrochem 25:155
20. Trasatti S (1984) Electrochim Acta 29:1503
21. Mozota J, Conway BE (1991) J Electrochem Soc 128:2142
22. Snoeyink VL, Jenkins D (1980) Water chemistry. John Wiley & Sons, New York, p 386
23. Stum W, Morgan JJ (1996) Aquatic chemistry, 3rd edn. John Wiley & Sons, New York, Chap. 8, p 490
24. Callaway JO (1989) In: Clesceri LS, Greenberg AE, Trussel RR (eds) Standard methods for the examination of water and wastewater, 17th edn. Alpha Awwa-WPCF, Washington, DC, Part 4000, p 62
25. Spyrkowicz L, Kaul SN, Neti RN, Satyanarayan S (2005) Water Res 39:1601
26. Spyrkowicz L, Radaelli M, Daniele S (2005) Catal Today 100:425
27. Vlyssides AG, Loizidou M, Karis PK, Zorpas AA, Papaioannou D (1999) J Hazard Mater B70:41
28. Comninellis Ch, Pulgarin C (1993) J Appl Electrochem 23:108
29. Comninellis Ch (1994) Electrochim Acta 39:1857
30. Fugivara PTA, Cardoso AA, Benedetti AV (1996) Analyst 121:541
31. Iwakura C, Sakamoto K (1985) J Electrochem Soc 132:2420
32. Carneiro PA, Osugi ME, Fugivara CS, Borale N, Zanoni MVB (2005) Chemosphere 59:431
33. Hepel M, Luo J (2001) Electrochim Acta 47:729
34. Zollinger H (1991) Color chemistry: syntheses, properties and applications of organic dyes and pigments, 2nd edn. V.C.H. Publishers, New York
35. Forti JC, Olivi P, Andrade AR (2004) J Electrochemical Soc 150:E222
36. Ortiz PI, De Pauli CP, Trasatti S (2004) J New Mater Electrochem Syst 7:153
37. Vogel AI (1995) Qualitative analytical chemistry, 5th edn. Mestre Jou Publishers, São Paulo, p 419
38. Cachet H, Zenia F, Froment M (1999) J Electrochem Soc 146:977